

Liquefaction hazard assessment in a GIS environment: A case study of Buğday Pazarı neighborhood in Çankırı province

Eren Yurdakul¹, Şevki Öztürk*² and Ender Sarıfakıoğlu¹

¹Department of Civil Engineering, Çankırı Karatekin University, UluYazı Campus, 18100, Çankırı, Türkiye

²Department of Civil Engineering, Çankaya University, Central Campus, 06790, Etimesgut, Ankara, Türkiye

(Received June 8, 2023, Revised October 27, 2023, Accepted February 15, 2024)

Abstract. Seismic movements have varying effects on structures based on characteristics of local site. During an earthquake, weak soils are susceptible to damage due to amplified wave amplitudes. Soil-structure interaction issue has garnered increased attention in Türkiye, after devastating earthquakes in Kocaeli Gölçük (1999), İzmir (2020), Kahramanmaraş Pazarcık and Elbistan (2023). Consequently, liquefaction potential has been investigated in detail for different regions of Türkiye, mainly with available field test results. Çankırı, a city located close to North Anatolian Fault, is mainly built on alluvium, which is prone to liquefaction. However, no study on liquefaction hazard has been conducted thus far. In this study, groundwater level map, SPT map, and liquefaction risk map have been generated using Geographical Information System (GIS) for the Buğday Pazarı District of Çankırı province. Site investigations studies previously performed for 47 parcels (76 boreholes) were used within the scope of this study. The liquefaction assessment was conducted using Seed and Idriss's (1971) simplified method and the visualization of areas susceptible to liquefaction risk has been accomplished. The results of this study have been compared with the City Council's precautionary map which is currently in use. As a result of this study, it is recommended that minimum depth of boreholes in the region should be at least 30m and adequate number of laboratory tests particularly in liquefiable areas should be performed. Another important recommendation for the region is that detailed investigation should be performed by local authorities since findings of this study differ from currently used precautionary map.

Keywords: alluvium; geographical information system; liquefaction; liquefaction hazard assessment; site characterization

1. Introduction

All engineering structures interact with the ground in a way that some structures are built entirely within the ground, while others interact with it. For this reason, the interaction between the building and the underlying soil must be handled sensitively. The concentration of earthquake effects in specific areas has highlighted the explicit importance of soil characteristics. The varying ground conditions in regions located close to each other may result in significant differences in the recorded accelerations during an earthquake. Thus, the dynamic behavior of soils plays a crucial role in determining the effect on transmitted motion (Afacan and Güler 2019). Local site characteristics, including soil classification, play a critical role in identifying weak soil areas that are prone to geotechnical problems, such as bearing capacity, settlement, swelling, and collapse. Additionally, liquefaction is another significant problem that may occur under dynamic loads.

Liquefaction is the process where soil particles change from solid to liquid state due to increased pore water pressure and a decrease in effective stress. This is caused by the tendency of granular materials to compact when subjected to cyclic shear stresses, which increases the pore

water pressure and decreases intergranular effective stress (Sen 2009, Terzaghi *et al.* 1996). Earthquake-induced soil liquefaction is considered one of the most destructive natural hazards. Placing the piles in liquefiable soil that might become unstable under seismic loads is one of the major reasons for the failure of structures and infrastructure, such as bridges on pile foundations (Ebadi-Jamkhaneh *et al.* 2021). Moreover, although there have been many advancements in seismic codes, structures on shallow foundations resting on saturated sandy soil have still experience excessive settlement, rotation, or even tilting due to liquefaction during major seismic events (Kassas *et al.* 2022). Consequently, liquefaction remains a significant topic in the literature, and is still being studied in various ways.

Although the liquefaction of alluvial soil layers and its role in damages have been known for a long time, it has gained increased attention in Türkiye after the Kocaeli Gölçük earthquake in 1999, and the more recent earthquakes in İzmir in 2020 and Kahramanmaraş Pazarcık and Elbistan in 2023. During these earthquakes, structures built on alluvial deposits suffered severe damage due to liquefaction. Total collapse or tilting of structures and large amount of ground settlements were observed after all these earthquakes due to ground conditions. The most recent earthquakes occurred in Pazarcık and Elbistan resulted in major geotechnical problems such as foundation failures, lateral spreading, rock falls, landslides, and surface manifestations of liquefaction in alluvial regions. Similarly,

*Corresponding author, Ph.D.

E-mail: sevkiozturk@cankaya.edu.tr

the study area (Buğday Pazarı settlement) which rests on quaternary alluvial deposits formed by Acı and Tatlı streams (Akyürek *et al.* 1980, Hakyemez *et al.* 1986) and is characterized by sandy-gravelly-silty-clayey units and shallow ground water levels, is particularly vulnerable. Large-magnitude earthquakes in the region with shallow ground water levels and sandy-non-plastic silty units can significantly increase the risk of liquefaction in this area. This issue is the subject of ongoing research.

The field tests are commonly used for liquefaction potential assessment in geotechnical engineering studies. The standard penetration test (SPT), the cone penetration test (CPT), and measurement of shear wave velocity (V_s) are the most common methods to estimate the liquefaction potential of soil (Youd *et al.* 2001). SPT is generally preferred over others to evaluate the liquefaction in most of the studies (Tunusluoglu and Karaca 2018). There are many liquefaction hazard assessment studies executed throughout Türkiye (Esin and Ceryan 2015, Isik *et al.* 2016, Dipova and Cangir 2017, Tunusluoglu and Karaca 2018, Akın 2019, Silahtar *et al.* 2020, Sengül and Karabas 2021, Günes and Ekmen 2022, Acar and Kaya 2023, Silahtar *et al.* 2023). In these studies, liquefaction potential has been investigated in detailed for different regions of Türkiye as well as Seed and Idriss (1971), Iwasaki *et al.* (1982), Youd *et al.* (2001), Yılmaz and Cetin (2004), Sonmez and Gokceoglu (2005), Kayen *et al.* (2013) methods have been used.

According to the author's knowledge, there has been no such study processed in Çankırı province yet and it is a critical deficiency in disaster planning of the city. The main objective of this study is to address this gap by creating a risk map using a GIS program to identify weak soil areas where liquefaction problems may occur based on the ground survey results obtained in the past. In the study, the liquefaction assessment was conducted using Seed and Idriss's (1971) "simplified method". In this context, previously performed site studies (boreholes and geophysical studies in 47 parcels (76 boreholes) in Buğday Pazarı Neighborhood) and laboratory experiments related to these site studies were examined in detail within the scope of this study. The results of the study were visualized in the GIS environment. It is expected that the resulting recommendations will influence city planning decisions.

2. Study area

Çankırı province is located between the Central Kızılırmak Section of the Central Anatolian Region and the western section of the Black Sea region as shown in Fig. 1.

The city has a surface area of 7490 km². The province of Çankırı is adjacent to the provinces of Kastamonu, Karabük, Kırıkkale, Çorum, Bolu and Ankara. The province is situated in the geographic coordinates of 41° 04' north to 40° 16' south latitude and 34° 08' east to 32° 34' west longitude. The province of Çankırı has a north-south length of approximately 90 km and an east-west length of about 126 km (Ates *et al.* 2008). The study area is Buğday Pazarı Neighborhood, which is the most densely populated residential area of the central district in terms of population

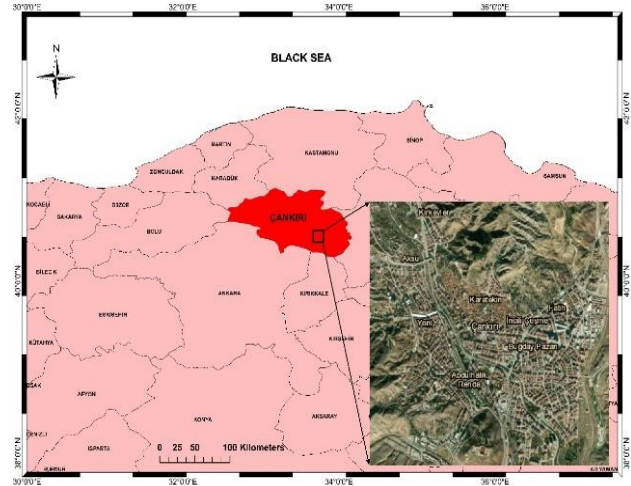


Fig. 1 Location map of the study area

Table 1 Population of districts (TUIK 2022)

Neighborhood	Population
Buğday Pazarı	26968
Abdulhalik Renda	19087
Aksu	9209
Fatih	8535
Yeni	8279
Kırkevler	7618
Others	11687

according to the 2022 census data from TUIK shown in Table 1.

3. Geological and hydrogeological features

A compressional tectonic regime caused by the strike-slip faults formed from the Pliocene to the present day, played an important role in the formation of the region. The Çankırı basin is located among the Eldivan Mountain in the west, the Ilgaz Mountain-Yapraklı Mountain in the north, and the Köse Mountain in the east. The Çankırı basin is qualified as the intermountain basin (Tuysuz and Dellaloglu 1992).

In the Middle Eocene (45 million years ago), the Neo-Tethys Ocean closed because of the collision of the Sakarya and Kırşehir microcontinents. During the Middle-Late Eocene, shallow marine sediments were deposited, and volcanism was active. The collision of continents and thickening rock units formed mountain belts. Due to the orogenic collapse caused by the extensional tectonic regime from Oligo-Miocene to Pliocene, Oligo-Miocene aged the Incik formation, which represents the clastic rocks of the fluvial environment as terrestrial sediments of the Çankırı basin, is observed onto the remnant slices of the oceanic lithosphere. The Upper Miocene aged the Bayındır Formation consists of gypsum, mudstone and sandstone succession and indicates a closed lake basin environment.

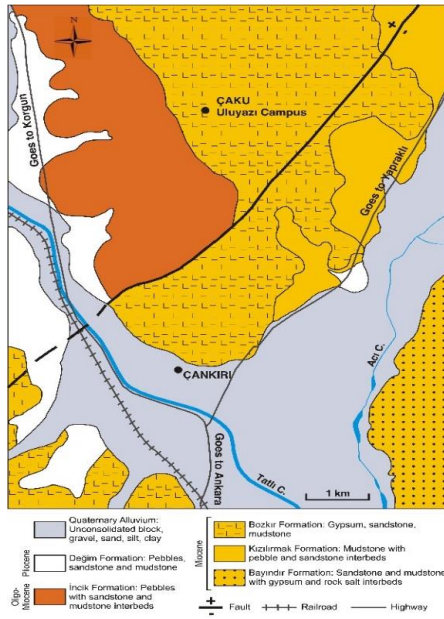


Fig. 2 Geological map of Çankırı (modified from Ateş *et al.* 2008)

The Kızılırmak Formation, which consists of red colored mudstone, sandstone, and conglomerate, is transitional between the Bayındır formation and the overlying the Bozkır formation. The Upper Miocene-Lower Pliocene Bozkır formation was deposited in a lacustrine evaporitic environment and mainly includes gypsum, mudstone, and sandstone levels. The Upper Pliocene aged the Değim Formation consists of burgundy, brown colored conglomerate, mudstone, and a small amount of sandstone. The youngest units of the basin are the Quaternary alluviums formed by Acı and Tatlı streams (Akyürek *et al.* 1980, Hakyemez *et al.* 1986). The majority of the settlement area is covered with liquefiable Quaternary alluvial sediments. The geological map of the region is shown in Fig. 2.

It is commonly known that the geological characteristics at the building's site affect the earthquake shaking (Jakka *et al.* 2015). Besides, the spatial distribution of the groundwater level in the region, which may cause favorable conditions for liquefaction potential, is of great importance. Several works have shown the shallow ground water level and the presence of alluvial soils raise the liquefaction potential (Johnston and Schweig 1996, Kayen and Mitchell 1997, Frankel *et al.* 2002, Duman *et al.* 2014). Groundwater level data in the study area is visualized in Fig. 3. It is seen that the groundwater level varies between 0.7 m and 6 m in most of the study area, though it reaches up to 10 m depth at north-west points.

4. Tectonic features

The Anatolian microplate shifts westward at an average rate of 24 mm/year along conjugate intra-continental strike-slip faults of the right-lateral North Anatolian Fault Zone

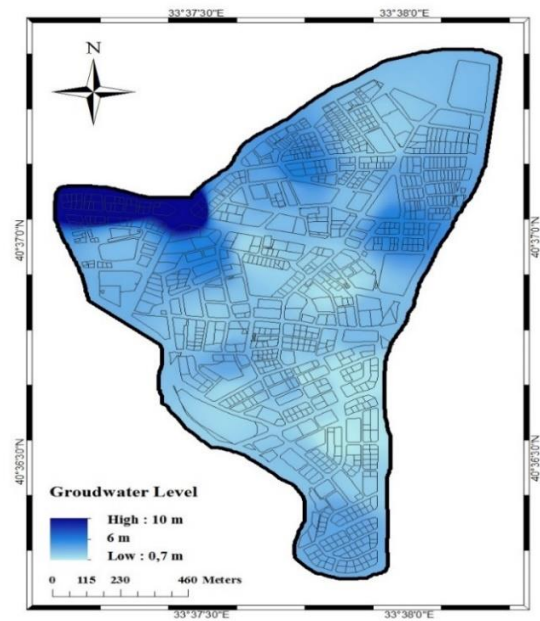


Fig. 3 Groundwater level map

(NAFZ) and the left-lateral East Anatolian Fault Zone (EAFZ). The study area shown in Fig. 4 is located just south of the North Anatolian Fault (NAF) (Ketin 1976).

Çankırı province, which is very close to the North Anatolian Fault Zone, was greatly affected by the Ladik-Tosya earthquake that occurred on November 26, 1943, with a magnitude of $M_s = 7.2$ (Alsan *et al.* 1976). Orta Fault is a north-south trending, west dipping reverse component left lateral strike-slip fault located in the western part of Orta district. An earthquake of magnitude $M_w = 6.0$ struck on June 6, 2000. The Çankırı Fault, which is one of the most important faults in Çankırı province, borders the Çankırı Basin from the west and east, in a north-northeast-southwest direction, dipping to the west-northwest. This fault, which is an active unit today, has a total length of 73 km and has the potential to produce an earthquake with a magnitude of $M_w = 7.27$ (AFAD 2021).

Large earthquakes are historically known and expected in the area because it is known to be seismically active. The figure of the quake (1940-2023) epicenters in Çankırı and its vicinity is shown in Fig. 5.

5. Materials and methods

Site investigations studies previously performed for 47 parcels located within the borders of Buğday Pazarı Neighborhood were obtained from Çankırı Municipality Directorate of Reconstruction and Urbanization and were employed within the scope of the study (Fig. 6). There is no available information in the industrial parcels located at the northeastern end of the neighborhood.

To evaluate the liquefaction susceptibility, the widely used methodology was proposed by Seed and Idriss (1971) called "simplified procedure" Eq. (1). This method was then

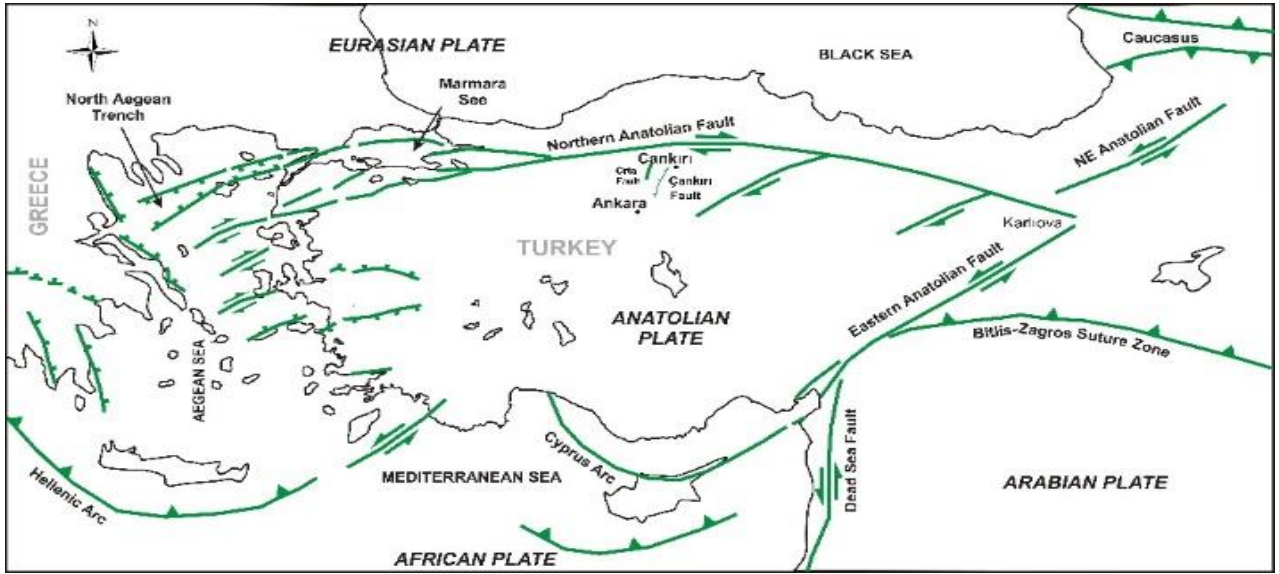


Fig. 4 Türkiye's main fault belts

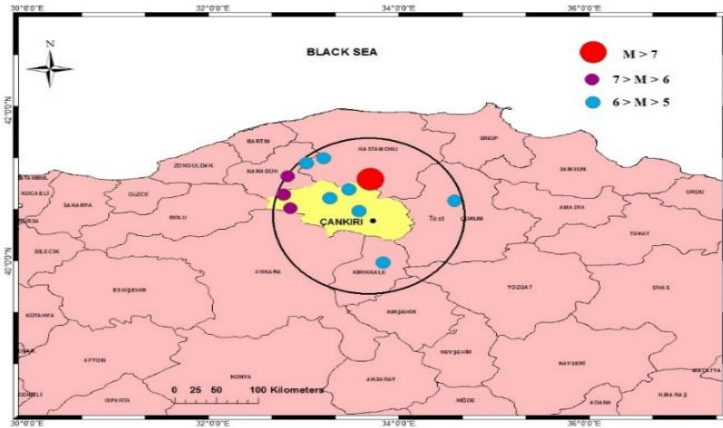


Fig. 5 Çankırı and its vicinity, quakes of Mw=5.5 and above (modified from AFAD 2023)

modified by Seed *et al.* (1985) and Youd *et al.* (2001). The method utilizes the calculation of the ratio between cyclic resistance ratio (CRR) Eq. (2) and the cyclic stress ratio (CSR) Eq. (4), to determine the safety factor (FS) against liquefaction. This method is employed based on SPT-N data. The CRR is computed by the following equation

$$FS = \frac{CRR}{CSR} \quad (1)$$

$$CRR = \frac{1}{34 - N_{1,60cs}} + \frac{N_{1,60cs}}{135} + \frac{50}{[10N_{1,60cs} + 45]^2} - \frac{1}{200} \quad (2)$$

Certain corrections are applied to the raw SPT values (N) obtained from the research data. $N_{1,60}$ is the corrected penetration resistance ($N_{1,60} = N * C_N * C_R * C_S * C_B * C_E$) depends on the overburden pressure factor (C_N), the hammer energy ratio (C_E), the borehole diameter (C_B), the rod length (C_R), and the correction for samplers with or without liners (C_S) (see Table 2). Finally, the equivalent clean sand value,

$N_{1,60cs}$, is obtained by applying a fine content correction using the equation Eq. (3) suggested by Youd and Idriss (1997) as detailed in Table 3. The corrected SPT-N values are visualized in Fig. 7. The SPT-N values in the study area range from 7 to 30. However, the analysis reveals that most of the SPT-N values in the study area are below 15.

$$N_{1,60cs} = \alpha + \beta(N_{1,60}) \quad (3)$$

Consequently, these weak soil areas are susceptible to not only liquefaction but also various geotechnical issues including bearing capacity problems, settlement, swelling and collapse.

The CSR is the seismic demand and computed by the following equation

$$CSR = 0.65 \left(\frac{a_{max}}{g} \right) \left(\frac{\sigma_{v0}}{\sigma'_{v0}} \right) r_d \quad (4)$$

where σ_{v0} and σ'_{v0} are the total vertical stress and the effective vertical stress at depth z , a_{max} is the peak

Table 2 SPT correction factors (Adopted from Skempton 1986)

Correction Factor	Equipment Variables	Correction Value
C_R	3-4 m	0.75
	4-6 m	0.85
	6-10 m	0.95
	>10 m	1.00
C_S	Standard sampler	1.00
	Sampler without liner	1.20
	65-115 mm diameter	1.00
C_B	150 mm diameter	1.05
	200 mm diameter	1.15
	Safety hammer	0.70-1.20
C_E	Donut hammer	0.50-1.00
	Automatic hammer	0.80-1.50

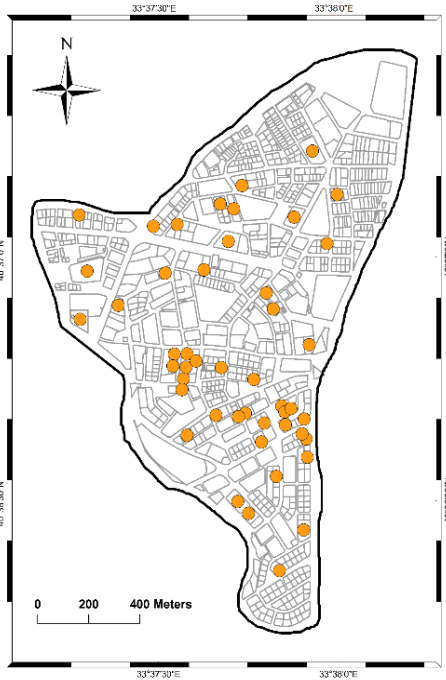


Fig. 6 Boring locations

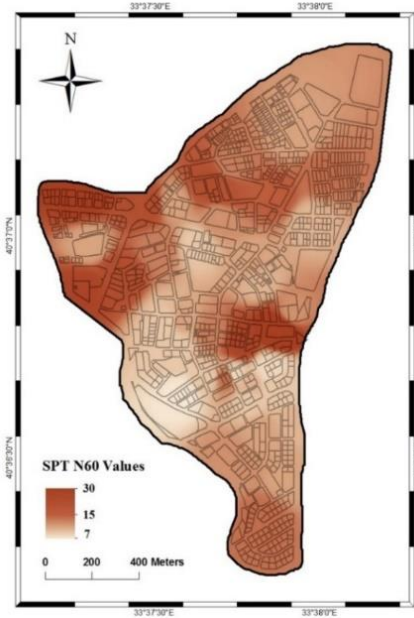


Fig. 7 SPT-N values map for the study area

Table 3 SPT correction factors based on fine content (%) (Seed *et al.* 1984)

Fine Content (FC)	α	β
FC ≤ % 5	$\alpha = 0$	$\beta = 1$
%5 < FC < %35	$\alpha = \exp [1.76 - (190/FC^2)]$	$\beta = 0.99 + FC^{1.5}/1000$
FC ≥ % 35	$\alpha = 5$	$\beta = 1.2$

horizontal ground acceleration, g is the gravitational acceleration, and r_d is the factor of stress reduction. The factor r_d is determined through the application of equations proposed by Liao and Whitman (1986). The final equation used in the calculation was proposed by Robertson and Wride (1998) given in Eq. (5). A sample calculation is given in Table 4 while the borehole locations and structures are given in Table 5.

$$\begin{aligned}
 r_d &= 1.000 - 0.00765z & z \leq 9.15 \text{ m} \\
 r_d &= 1.174 - 0.0267z & 9.15 \text{ m} < z \leq 23 \text{ m} \\
 r_d &= 0.744 - 0.008z & 23 \text{ m} < z \leq 30 \text{ m}
 \end{aligned} \tag{5}$$

For magnitudes both greater and less than 7.5, the CSR values have been divided by the magnitude scaling factor (MSF), which is calculated using the Eq. (6) proposed by

Seed and Idriss (1982). For $M_w = 7.5$, the MSF is equal to 1. Çankırı experienced significant impacts from the Ladik-Tosya earthquake which had a magnitude of $M_s = 7.2$ on November 16, 1943. To ensure a conservative approach in the liquefaction evaluation analysis, $M_w = 7.5$ was used in the calculations, prioritizing safety precautions.

$$MSF = \frac{10^{2.24}}{M_w^{2.56}} \tag{6}$$

Table 4 Sample calculation for a typical borehole in Seed and Idriss's Simplified Procedure (1971)

Depth (m)	Unit Weight (kN/m ³)	r_d	FC (%)	PI	C_N	$N_{1,60}$	α	β	$N_{1,60cs}$	CRR	MSF	CSR	FS	Comment
1.5	18.8	0.989	32	12	1.700	19	4.8	1.2	27.2	0.34	1.0	0.22	1.58	Not Susceptible
3.0	18.8	0.977	26	7	1.338	15	4.4	1.1	21.3	0.23	1.0	0.22	1.08	Susceptible
4.5	18.8	0.966	28	11	1.126	11	4.5	1.1	17.0	0.18	1.0	0.23	0.80	Susceptible
6.0	18.8	0.954	37	9	1.043	13	5.0	1.2	20.0	0.22	1.0	0.26	0.84	Susceptible

During the analyses of geotechnical data, a GIS program has been utilized for presenting these data in a more easily comprehensible manner through thematic maps. First of all, the borehole locations were defined within the program. Then, SPT data, ground water data, and results of liquefaction analyses were entered to related locations. The data entered on a parcel-specific basis has been transformed into neighborhood-level result. The technical role of GIS program was regarding spatial distribution of liquefaction susceptibility through the study area by using interpolation technique. It should be duly noted that in maps generated using interpolation, the non-uniform distribution of boreholes in the region can potentially introduce certain ambiguities into the results.

6. Results and discussion

$$FS = \frac{CRR}{CSR} \geq 1.10 \quad (7)$$

The liquefaction state is classified as "no liquefaction" when the condition defined in Eq. (7) is satisfied, while it is categorized as "liquefaction exists" when the condition is not satisfied. However, it is quite important to underline that soils with high cohesion or low cohesion and plasticity index (PI) greater than 12 are not expected to experience liquefaction. On the other hand, low plasticity or non-plastic silts and silty sands are considered the most susceptible to liquefaction hazards (Seed *et al.* 2003). In loose to medium dense specimens, the presence of fines considerably affected the undrained cyclic response, however at extremely high relative densities, it was shown to be independent of silt content (Dash and Sitharam 2011). Research findings demonstrated that the liquefaction potential of the sand rises as the mean grain falls (Molina-Gomez *et al.* 2020, Sonmezer *et al.* 2020). Also, the liquefaction potentials of coarse-grained sands rise with increasing silt concentration (Sonmezer *et al.* 2022). The study area is quite vulnerable due to its sandy-gravelly-silty-clayey units and shallow ground water levels.

The distribution of liquefaction risk conditions in the study area is depicted in Fig. 8, based on the liquefaction analysis for the soil layers b/w 3-6 m depths due to limited number of laboratory data. There is a risk of liquefaction in large part of the parcels (54% of the study area) represented by red colors within the boundaries of the Buğday Pazarı

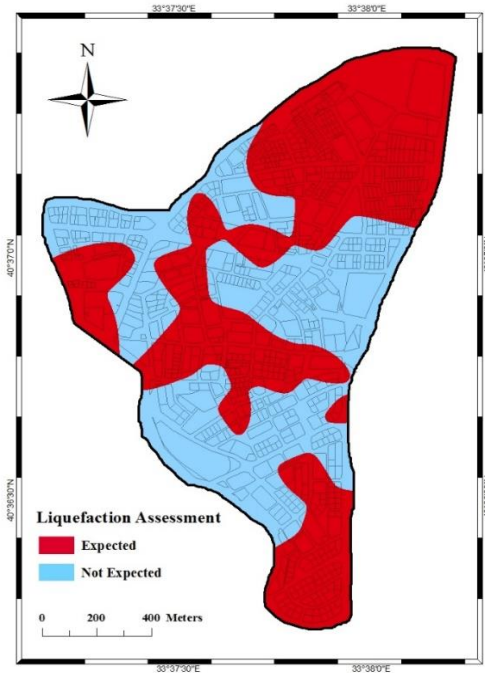


Fig. 8 Liquefaction risk map

District. Based on the analysis conducted using the simplified procedure, the regions colored in blue indicate a lack of liquefaction risk.

Evaluating Figs. 3-7-8 altogether, the liquefaction prone areas are characterized with shallow groundwater levels ranging from 0.7 m to 6 m and SPT-N values below 15.

In accordance with the decision of Çankırı Municipality Council, Buğday Pazarı Neighborhood has been assigned as a Special Project Area and the lithology-based precaution suggestions for the region is shown in Fig. 9. As indicated in the figure, the study area classified as medium to very compact alluvial soil (11%), loose-soft alluvial (37%), and prone to liquefaction (52%).

Additionally, Fig. 10 presents the overlay of the liquefaction risk map generated by this study and the precautionary areas designated by the City Council. It must be highlighted that there is some disparity between the findings of this study and the current precautionary map of the city regarding the projection of liquefaction risk. According to the research findings, liquefaction risk is not expected in 45% of the area that is classified as prone to liquefaction. On the other hand, in 51% of the area where

Table 5 Borehole (BH) locations and structures

BH No	Coordinates		BH Depth (m)	GW Depth (m)	Description
	Lat (N)	Long (E)			
BH 1	40.5945	33.6251	10.5	4	silty sandy clay with clayey sand intermediate levels
BH 2	40.5943	33.6256	10.5	4	silty sandy clay with clayey sand intermediate levels
BH 3	40.5933	33.6251	10.5	2.5	clayey silty sand with sandy clay and silty clay intermediate levels
BH 4	40.5935	33.6256	10.5	2.5	clayey silty sand with sandy clay and silty clay intermediate levels
BH 5	40.5927	33.6272	10.5	1.3	gravelly sandy clay with clayey silty sand intermediate levels
BH 6	40.5928	33.6268	10.5	1.3	gravelly sandy clay with clayey silty sand intermediate levels
BH 7	40.5934	33.6258	12	3	fine units, brown silty clay
BH 8	40.5936	33.6254	12	3	fine units, brown silty clay
BH 9	40.5932	33.6281	12	3	fine units, brown silty clay
BH 10	40.5936	33.6280	10.5	1	clayey silty sand with sandy clay and silty clay intermediate levels
BH 11	40.5933	33.6282	10.5	1	clayey silty sand with sandy clay and silty clay intermediate levels
BH 12	40.5934	33.6281	10.5	1	sandy silty clay with sandy gravel intermediate levels
BH 13	40.5932	33.6283	10.5	1	sandy silty clay with sandy gravel intermediate levels
BH 14	40.5932	33.6308	10.5	1	sandy silty clay with sandy gravel intermediate levels
BH 15	40.5929	33.6311	10.5	1	sandy silty clay with sandy gravel intermediate levels
BH 16	40.5932	33.6312	10.5	1	sandy silty clay with sandy gravel intermediate levels
BH 17	40.5938	33.6303	10.5	1	sandy silty clay with sandy clay and gravelly clay units
BH 18	40.5937	33.6299	10.5	1	sandy silty clay with sandy clay and gravelly clay units
BH 19	40.5934	33.6299	10.5	1	sandy silty clay and gravelly clay units
BH 20	40.5935	33.6302	10.5	1	sandy silty clay and gravelly clay units
BH 21	40.5937	33.6301	10.5	1	sandy silty clay and gravelly clay units
BH 22	40.5938	33.6303	10.5	1	sandy silty clay and gravelly clay units
BH 23	40.5924	33.6307	10.5	1.5	clayey silty sand and sandy silty gravelly clay units
BH 24	40.5926	33.6304	10.5	1.5	clayey silty sand and sandy silty gravelly clay units
BH 25	40.5929	33.6291	10.5	1.5	silty sandy clay with sandy clayey gravel intermediate levels
BH 26	40.5928	33.6290	10.5	1.5	silty sandy clay with sandy clayey gravel intermediate levels
BH 27	40.5928	33.6312	10.5	1	clayey sandy silt and sandy silty gravelly clay units
BH 28	40.5929	33.6310	10.5	1	clayey sandy silt and sandy silty gravelly clay units
BH 29	40.5926	33.6308	10.5	1	clayey sandy silt and sandy silty gravelly clay units
BH 30	40.5928	33.6312	10.5	1.5	clayey sandy silt and sandy silty gravelly clay units
BH 31	40.5924	33.6311	10.5	1.5	clayey sandy silt and sandy silty gravelly clay units
BH 32	40.5922	33.6310	10.5	1	sandy silty gravelly clay
BH 33	40.5920	33.6313	10.5	1	sandy silty gravelly clay
BH 34	40.5885	33.6297	13	4	fine units, brown silty clay
BH 35	40.5879	33.6298	13	4	fine units, brown silty clay
BH 36	40.5882	33.6303	13	4	fine units, brown silty clay
BH 37	40.5882	33.6294	13	4	fine units, brown silty clay
BH 38	40.5883	33.6300	13	4	fine units, brown silty clay
BH 39	40.5994	33.6323	10.5	6	sandy silty clay with sandy gravel units
BH 40	40.5992	33.6321	10.5	6	sandy silty clay with sandy gravel units
BH 41	40.6008	33.6326	13	4	fine units, brown silty clay

Table 5 Continued

BH No	Coordinates		BH Depth (m)	GW Depth (m)	Description
	Lat (N)	Long (E)			
BH 42	40.6012	33.6325	13	4	fine units, brown silty clay
BH 43	40.6009	33.6328	13	4	fine units, brown silty clay
BH 44	40.5951	33.6274	10.5	2.5	sandy gravel and clayey gravelly sand units with sandy gravelly clay units
BH 45	40.5950	33.6271	10.5	2.5	sandy gravel and clayey gravelly sand units with sandy gravelly clay units
BH 46	40.5970	33.6296	10.5	1	clayey silty sand and sandy gravel units with silty gravelly sandy clay levels
BH 47	40.5971	33.6297	10.5	1	clayey silty sand and sandy gravel units with silty gravelly sandy clay levels
BH 48	40.6012	33.6280	15.5	6	silty clay with clayey sandy gravel levels
BH 49	40.6014	33.6283	15.5	6	silty clay with clayey sandy gravel levels
BH 50	40.5975	33.6294	10.5	2	sandy gravel and clayey gravelly sand units with sandy gravelly clay units
BH 51	40.5978	33.6293	10.5	2	sandy gravel and clayey gravelly sand units with sandy gravelly clay units
BH 52	40.6010	33.6277	10.5	4	sandy gravelly clay
BH 53	40.6004	33.6277	10.5	4	sandy gravelly clay
BH 54	40.6001	33.6282	10.5	4	sandy gravelly clay
BH 55	40.5961	33.6310	10.5	3	sandy silty gravelly clay units with sandy gravel intermediate levels
BH 56	40.5957	33.6315	10.5	3	sandy silty gravelly clay units with sandy gravel intermediate levels
BH 57	40.5955	33.6313	10.5	3	sandy silty gravelly clay units with sandy gravel intermediate levels
BH 58	40.6008	33.6275	10.5	4	sandy gravelly clay
BH 59	40.6006	33.6270	10.5	4	sandy gravelly clay
BH 60	40.6007	33.6275	10.5	4	sandy gravelly clay
BH 61	40.6001	33.6254	12	2	sandy gravelly clay with clayey sand intermediate levels
BH 62	40.5999	33.6252	12	2	sandy gravelly clay with clayey sand intermediate levels
BH 63	40.5972	33.6222	16	2	fine units, brown silty clay with coarse units, light brown gravel-sand-clay mixtures
BH 64	40.5972	33.6227	16	2	fine units, brown silty clay with coarse units, light brown gravel-sand-clay mixtures
BH 65	40.5985	33.6249	10.5	6	gravelly sandy clay with clayey sandy gravel intermediate levels
BH 66	40.5981	33.6245	10.5	6	gravelly sandy clay with clayey sandy gravel intermediate levels
BH 67	40.5943	33.6256	10.5	3.5	silty sandy gravelly clay with silty clayey sand units
BH 68	40.5942	33.6252	10.5	3.5	silty sandy gravelly clay with silty clayey sand units
BH 69	40.5986	33.6203	25	3	silty clay with gravelly silty sand units
BH 70	40.5981	33.6204	25	3	gravelly sandy silty clay with gravelly sand units
BH 71	40.5980	33.6209	25	3	clayey gravelly sand with silty clay and silt units
BH 72	40.5981	33.6217	25	3	clayey gravelly sand with clayey silt units
BH 73	40.5988	33.6218	25	3	brown silty sand with clay intermediate levels
BH 74	40.5988	33.6215	25	3	light brown silty sand and gravel with clay and silt levels
BH 75	40.5988	33.6212	25	3	clayey silt and sand units with sandy silty clay levels
BH 76	40.5985	33.6202	25	3	clayey silty gravelly sand with silty sandy clay units

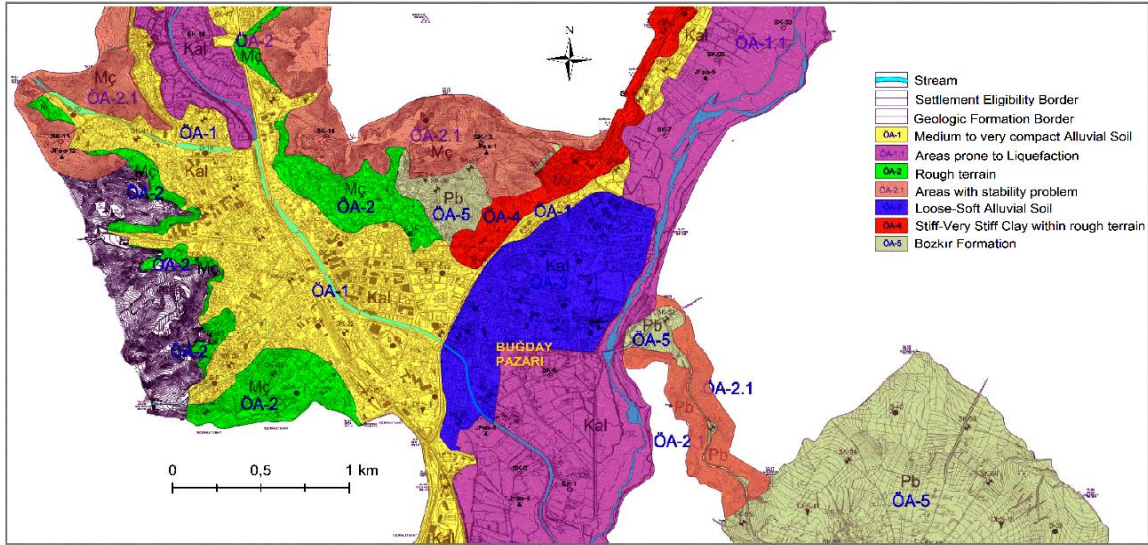


Fig. 9 Precautionary areas map in accordance with the decision of Çankırı Municipality Council

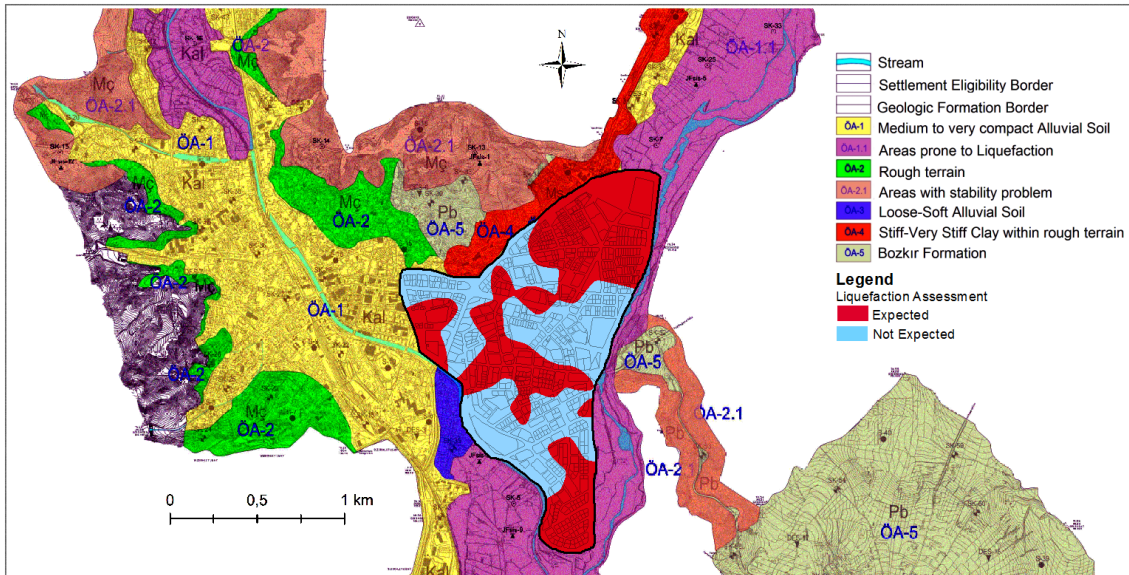


Fig. 10 Superimposed view of liquefaction risk map and precautionary areas map

liquefaction risk is not expected on the map, the liquefaction risk has actually been determined. Ultimately, the study results and the precautionary map outcomes are parallel in 47.5% of the entire area.

7. Conclusions

This study has revealed the liquefaction risk present in the Buğday Pazarı Neighborhood, which is the largest settlement area of Çankırı. The district is situated on quaternary deposits and is located in close proximity to the North Anatolian Fault line, making it highly susceptible to liquefaction hazards. By utilizing 47 parcels (76 borehole) data and geotechnical reports from Çankırı Municipality Directorate of Reconstruction and Urbanization, a liquefaction risk map was developed using a GIS program

in order to identify areas with weak soil conditions issue could potentially arise.

On the other hand, some specific limitations were encountered during the liquefaction analyses conducted for the related region. Firstly, almost all boring depths were limited to 10.5 m. Secondly, available laboratory data was quite rare which is at two different depths along a 10.5 m depth on average. Also, ground water levels were considered as stable during analyses and seasonal fluctuations were neglected. These limitations may affect the reliability of the results.

Despite these limitations, the study has revealed usable implications as follows. There are settlements within the area that are at risk of liquefaction, characterized with shallow groundwater levels ranging from 0.7 m to 6 m and SPT-N values below 15. Particularly in the northern and southern parts of the neighborhood, there are residential

areas that exhibit a high potential for liquefaction, drawing attention throughout the district. In these regions, there is a significant risk of damage resulting from liquefaction during high-magnitude seismic events.

Unfortunately, Türkiye has recently experienced a disaster due to Pazarcık (7.7) and Elbistan (7.6) earthquakes, resulting in the loss of more than 50,000 lives. Some residential buildings toppled in an exceptional case of liquefaction-induced bearing capacity collapse (Cetin *et al.* 2023). The settlement area of Çankırı bears a striking resemblance in terms of liquefaction potential to those cities that were severely impacted by the disaster. Since it is experienced the extent of destruction by a major earthquake in Pazarcık and Elbistan, several recommendations have been proposed to avoid facing similar situations in the future for the Çankırı region. These suggestions are related with conducting suitable geotechnical investigations and performing appropriate ground improvement techniques. It is recommended to drill boreholes with a minimum depth of 30 m and conduct an adequate number of laboratory tests, particularly in areas highlighted on the maps where liquefaction is likely to occur. Based on the liquefaction risk map obtained from the study, it is advised to permit high-rise constructions in areas with a high liquefaction risk, only if necessary technical precautions are implemented. By this way, it is predicted that the risk of liquefaction will be reduced, and undesirable situations will not be encountered for further constructions within the area.

There is a liquefaction potential in most (54%) of the district based on the study findings. The research's findings indicate that liquefaction danger is not anticipated in 45% of the region designated on the precautionary map as prone to liquefaction. On the other hand, the liquefaction danger has been established in 51% of the region where it is not anticipated on the map. Ultimately, %47.5 of the overall region shows comparable results between the research and the precautionary map. Since there are significant points where liquefaction risk exists but have not been projected by the municipality and vice versa, detailed study should be performed by local authorities and the distinctness should be analyzed thoroughly by further studies.

The findings of this research can be improved at a future date after a detailed geotechnical investigation in some parts of the region with boreholes having adequate lengths and conducting more frequent laboratory tests on the samples taken at appropriate depths along the boreholes.

As a pioneering study in Çankırı, it is anticipated that this research will make a valuable contribution to the existing literature on liquefaction analysis and mitigation measures. This research will enable engineers to give the special importance to geotechnical investigations. Also, it will allow liquefaction analyses to be carried out in more detail. It will guide decision-makers correctly when determining zoning areas.

References

Acar, M.C. and Kaya, D. (2023), "Geographic information system approach in evaluating the geotechnical properties of soils: A case study of Oymaağaç in Kayseri", *J. Fac. Eng. Architect.*

- Gazi Univ.*, **38**(2), 1079-1092. <https://doi.org/10.17341/gazimmfd.946963>.
- Afacan, B. and Güler, E. (2019), "Performance of new Turkish building code determination by soil amplification analysis", *Proceedings of the International Conference on Earthquake Engineering and Seismology*, Ankara, Türkiye, October.
- AFAD. (2021), "İRAP II Afet Risk Azaltma Planı Hazırlama Kılavuzu", Ministry of Interior Disaster and Emergency Management Presidency.
- AFAD (2023), Deprem Kataloğu; Ministry of Interior Disaster and Emergency Management Presidency, Ankara, Türkiye. <https://deprem.afad.gov.tr/depremkatalogu>.
- Akın, M.K. (2019), "Düzce kent merkezi zeminlerinin sıvılaşma potansiyelinin değerlendirilmesi", *J. Geol. Eng.*, **43**(1), 39-56. <https://doi.org/10.24232/JMD.572465>.
- Akyürek, B., Bilginer, E., Çatal, E., Dager, Z., Soysal, Y. and Sunu, O. (1980), "Eldivan-Şabanözü (Çankırı), Hasayaz-Çandır (Kalecik-Ankara) dolayının jeolojisi", Research Report No. 6741; General Directorate of Mineral Research and Exploration, Ankara, Türkiye.
- Alsın, E., Tezuçan, L. and Bath, M. (1976), "An earthquake catalogue for Turkey for the interval 1913-1970", *Tectonophysics*, **31**(1-2). [https://doi.org/10.1016/0040-1951\(76\)90159-1](https://doi.org/10.1016/0040-1951(76)90159-1).
- Ates, S., Ozata, A., Gulmez, F., Osmancelebioglu, R., Mutlu, G., Ozerk, C., Yelezer, L. and Ustun, A.B. (2008), "Çankırı İli ve Kentsel Alanların (İl-İlçe Merkezleri) Yerbilim Verileri", Research Report No. 11098; General Directorate of Mineral Research and Exploration, Ankara, Türkiye.
- Cetin, K.O. and Ilgac, M. (2023), "Reconnaissance Report on February 6, 2023 Kahramanmaraş-Pazarcık (Mw=7.7) and Elbistan (Mw=7.6) Earthquakes", Türkiye Earthquake Reconnaissance and Research Alliance, Türkiye.
- Dash, H.K. and Sitharam, T.G. (2011), "Cyclic liquefaction and pore pressure response of sand-silt mixtures", *Geomech. Eng.*, **3**(2), 83-108. <https://doi.org/10.12989/gae.2011.3.2.083>.
- Dipova, N. and Cangir, B. (2017), "Lara - Kundu (Antalya) düzlüğünün sıvılaşma şiddeti indeksi'ne (LSI) dayalı sıvılaşma haritası", *J. Geol. Eng.*, **41**, 31-46. <https://doi.org/10.24232/JMD.311839>.
- Duman, E.S., İkizler, S.B., Angin, Z. and Demir, G. (2014), "Assessment of liquefaction potential of the Erzincan, Eastern Turkey", *Geomech. Eng.*, **7**(6), 589-612. <https://doi.org/10.12989/gae.2014.7.6.589>.
- Ebadi-Jamkhaneh, M., Homaioon-Ebrahimi, A., Kontoni, D.P.N. and Shokri-Amiri, M. (2021), "Numerical FEM assessment of soil-pile system in liquefiable soil under earthquake loading including soil-pile interaction", *Geomech. Eng.*, **27**(5), 465-479. <https://doi.org/10.12989/gae.2021.27.5.465>.
- Esin, G. and Ceryan, S. (2015), "Burhaniye (Balıkesir) yerleşim alanının sıvılaşma potansiyelinin değerlendirilmesi", *Yerbilimleri*, **36**(2), 81-96. <https://doi.org/10.17824/YRB.47475>.
- Frankel, A.D., Carver, D.L. and Williams, R.A. (2002), "Nonlinear and linear site response and basin effects in Seattle for the M 6.8 Nisqually, Washington, earthquake", *Bull. Seismol. Soc. Am.*, **92**(6), 2090-2109. <https://doi.org/10.1785/0120010254>.
- Günes, M. and Ekmen, A.B. (2022), "Yalova ili Süleymanbey mahallesinde bulunan proje alanının nonlineer sismik saha tepkisi kullanılarak sıvılaşma potansiyelinin incelenmesi", *Adıyaman Üniversitesi Mühendislik Bilimleri Dergisi*, **9**(17), 319-332. <https://doi.org/10.54365/ADYUMBD.1061896>.
- Hakyemez, Y., Barkurt, M.Y., Bilginer, E., Pehlivan, S., Can, B., Dager, Z. and Sozeri, B. (1986), "Yapraklı-İlgaz-Çankırı-Çandır Dolayının Jeolojisi", Research Report No. 7996; General Directorate of Mineral Research and Exploration, Ankara, Türkiye.
- Isık, A., Ünsal, N., Gürbüz, A. and Sisman, E. (2016), "Fethiye

- yerleşim alanındaki zeminlerin spt ve kayma dalga hızı verileriyle sıvılaşma potansiyelinin değerlendirilmesi”, *J. Fac. Eng. Architect. Gazi Univ.*, **31**(4), 1027-1037. <https://doi.org/10.17341/GAZIMMFD.278458>.
- Iwasaki, T., Tokida, K., Tatsuoka, F., Watanabe, S., Yasuda, S. and Sato, H. (1982), “Microzonation for soil liquefaction potential using simplified methods”, *Proceedings of the 3rd International Conference on Microzonation*, Seattle, USA, June.
- Jakka, R.S., Hussain, M. and Sharma, M.L. (2015), “Effects on amplification of strong ground motion due to deep soils”, *Geomech. Eng.*, **8**(5), 663-674. <https://doi.org/10.12989/gae.2015.8.5.663>.
- Johnston, A.C. and Schweig, E.S. (1996). “the enigma of the new madrid earthquakes of 1811-1812”, *Annu. Rev. Earth Pl. Sci.*, **24**, 339-384. <https://doi.org/10.1146/ANNUREV.EARTH.24.1.339>.
- Kassas, K., Adamidis, O. and Anastasopoulos, I. (2022), “Structure–soil–structure interaction (SSSI) of adjacent buildings with shallow foundations on liquefiable soil”, *Earthq. Eng. Struct. Dyn.*, **51**(10), 2315-2334. <https://doi.org/10.1002/EQE.3665>.
- Kayen, R.E. and Mitchell, J.K. (1997), “Assessment of liquefaction potential during earthquakes by arias intensity”, *J. Geotech. Geoenviron. Eng.*, **123**(12), 1162-1174. [https://doi.org/10.1061/\(ASCE\)1090-0241\(1997\)123:12\(1162\)](https://doi.org/10.1061/(ASCE)1090-0241(1997)123:12(1162)).
- Kayen, R., Moss, R.E.S., Thompson, E.M., Seed, R.B., Cetin, K. O., Kiureghian, A., Der, Tanaka, Y. and Tokimatsu, K. (2013), “Shear-wave velocity–based probabilistic and deterministic assessment of seismic soil liquefaction potential”, *J. Geotech. Geoenviron. Eng.*, **139**(3), 407-419. [https://doi.org/10.1061/\(ASCE\)GT.1943-5606.0000743](https://doi.org/10.1061/(ASCE)GT.1943-5606.0000743).
- Ketin, I. (1976), “San Andreas ve Kuzey Anadolu Fayları arasında bir karşılaştırma”, *Bull. Geol. Soc. Turkey*, **19**, 149-154.
- Liao, S.S.C. and Whitman, R.V. (1986), “Overburden correction factors for spt in sand”, *J. Geotech. Eng.*, **112**(3), 373-377. [https://doi.org/10.1061/\(ASCE\)0733-9410\(1986\)112:3\(373\)](https://doi.org/10.1061/(ASCE)0733-9410(1986)112:3(373)).
- Molina-Gómez, F., Viana da Fonseca, A., Ferreira, C. and Camacho-Tauta, J. (2020), “Dynamic properties of two historically liquefiable sands in the Lisbon area”, *Soil Dyn. Earthq. Eng.*, **132**, <https://doi.org/10.1016/J.soildyn.2020.106101>.
- Robertson, P.K. And Wride, C.E. (1998), “Evaluating cyclic liquefaction potential using the cone penetration test”, *Can. Geotech. J.*, **35**, 442-459. <https://doi.org/10.1139/T98-017>.
- Seed R.B., Cetin K.O., Moss R.E.S., Kammerer A.M., Wu J., Pestana J.M., Riemer M.F., Sancio R.B., Bray R.B., Kayen R.E. and Faris A. (2003), “Recent advances in soil liquefaction engineering: a unified and consistent framework”, Report No. EERC 2003–06, Earthquake Engineering Research Center, University of California, Berkeley, USA.
- Seed, H.B. and Idriss, I.M. (1971), “Simplified procedure for evaluating soil liquefaction potential”, *J. Soil Mech. Found. Division*, **97**(9), 1249-1273. <https://doi.org/10.1061/JSFEAQ.0001662>.
- Seed, H.B., Tokimatsu, K., Harder, L.F. and Chung, R.M. (1984), “The influence of SPT procedures in soil liquefaction resistance evaluations”, EERC Report No. UCB/EERC 84/15; Earthquake Engineering Research Center, University of California, Berkeley, USA.
- Seed H.B., Tokimatsu K., Harder L.F. and Chung R.M. (1985), “Influence of spt procedures in soil liquefaction resistance evaluations”, *J. Geotech. Eng.*, **111**(12), 1425-1445. [https://doi.org/10.1061/\(ASCE\)0733-9410\(1985\)111:12\(1425\)](https://doi.org/10.1061/(ASCE)0733-9410(1985)111:12(1425)).
- Sen, T.K. (2009), *Fundamentals of Seismic Loading on Structures*, John Wiley and Sons, West Sussex, United Kingdom.
- Sengül, T. and Karabas, B. (2021), “Kütahya merkez ilçesinde sıvılaşma potansiyelinin coğrafi bilgi sistemi ile incelenmesi”, *Bilecik Şeyh Edebali Üniversitesi Fen Bilimleri Dergisi*, **8**(2), 817-825. <https://doi.org/10.35193/BSEUFBD.962190>.
- Silahtar, A., Karaaslan, H., Ozocak, A., Bol, E., Sert, S., Kocaman, K. and Ozsagır, M. (2023), “Assessment of the liquefaction potential of the Arifiye (Sakarya) region with multidisciplinary geoscience approaches in the GIS environment”, *J. Appl. Geophys.*, **212**. <https://doi.org/10.1016/j.jappgeo.2023.104983>.
- Silahtar, A., Kanbur, M.Z. and Beyhan, G. (2020), “Investigation of a sedimentary basin by using gravity and seismic reflection data in the Isparta basin, southwestern Turkey”, *Bull. Eng. Geol. Environ.*, **79**(8), 3971-3988. <https://doi.org/10.1007/S10064-020-01804-Z>.
- Skempton, A.W. (1986), “Standard penetration test procedures and the effect in sands of overburden pressure, relative density, particle size, aging and over-consolidation”, *Geotechnique*, **36**, 425-447. <https://doi.org/10.1680/geot.1986.36.3.425>.
- Sonmez, H. and Gokceoglu, C. (2005), “A liquefaction severity index suggested for engineering practice”, *Environ. Geol.*, **48**, 81-91. <https://doi.org/10.1007/S00254-005-1263-9>.
- Sonmezer Y.B., Akyuz A. and Kayabali K. (2020), “Investigation of the effect of grain size on liquefaction potential of sands”, *Geomech. Eng.*, **20**(3), 243-254. <https://doi.org/10.12989/gae.2020.20.3.243>.
- Sonmezer Y.B., Kayabali K., Beyaz T. and Fener M. (2022), “Influence of grain size ratio and silt content on the liquefaction potentials of silty sands”, *Geomech. Eng.*, **31**(2), 167-181. <https://doi.org/10.12989/gae.2022.31.2.167>.
- Terzaghi, K., Peck, R.B. and Mesri, G. (1996), *Soil mechanics in engineering practice*, John Wiley and Sons Inc., New York, NY, USA.
- TUIK (2022), Biruni Adrese Dayalı Nüfus Kayıt Sistemi Sonuçları, Türkiye. <https://biruni.tuik.gov.tr/medas/?kn=95&locale=tr>.
- Tunusluoglu, M.C. and Karaca, O. (2018), “Liquefaction severity mapping based on SPT data: a case study in Canakkale city (NW Turkey)”, *Environ. Earth Sci.*, **77**(12), 422. <https://doi.org/10.1007/S12665-018-7597-X>.
- Tuysuz, O. and Dellaloglu, A.A. (1992), “Geologic evaluation of Çankırı basin and its tectonic units”, *Proceedings of the 9th Petroleum Congress of Türkiye*, Ankara, Türkiye, February.
- Yılmaz, Z. and Cetin K.O. (2004), “GIS-based seismic soil liquefaction assessment for Sakarya City after 1999 Kocaeli Turkey Earthquake”, *Proceedings of the 11th International Conference on Soil Dynamics and Earthquake Engineering*, U.C. Berkeley, CA, U.S.A, January.
- Youd, T.L. and Idriss I.M. (1997), “Proceedings of the NCEER workshops on evaluation of liquefaction resistance of soils”, Technical Report No. NCEER-97-0022; NCEER, Utah, USA.
- Youd, T. L., Idriss, I. M., Andrus, R.D. et al. (2001), “Liquefaction resistance of soils: summary report from the 1996 NCEER and 1998 NCEERNSF workshops on evaluation of liquefaction resistance of soils”, *J. Geotech. Geoenviron. Eng.*, **127**(10), 297-313. [https://doi.org/10.1061/\(ASCE\)1090-0241\(2001\)127:4\(297\)](https://doi.org/10.1061/(ASCE)1090-0241(2001)127:4(297)).